Cycle Slips Detection in Quad-Frequency Mode: Galileo's Contribution to an Efficient Approach under High Ionospheric Activity

CLGE Students' Contest 2014-2015

Galileo, EGNOS, Copernicus

Van de Vyvere, Laura

Université de Liège, Laura.VandeVyvere@alumi.ulg.ac.be

This paper is an abridged version of a part of the author's master thesis [Van de Vyvere, 2015], defended in June 2015 at Liège University, Belgium, under the supervision of Professor René Warnant. The full version is downloadable at *http://orbi.ulg.ac.be/handle/2268/184238*.

Abstract

Cycle slips detection has always been a key issue in phase measurements accuracy, thus impacting positioning precision. Since Galileo is the first constellation to offer four carrier frequencies available in *Open Service*, we were able to develop an innovative detection algorithm, especially promising in harsh environment like high ionospheric activity. This improves previous dual and triple-frequency methods, whose efficiency was somehow limited in tricky situations, like ionospheric events or particular configurations.

In our algorithm, two types of testing quantities were used: triple-frequency Simsky combination and dual-frequency Geometry-Free combination, each one being associated to a suitable detection algorithm. Simsky combination allows to detect almost every configuration, except for cycle slips of the same magnitude, appearing simultaneously on all carriers. Geometry-Free combination is only used to detect this particular case, since it suffers from quick variation of ionospheric delay. Together - through the choice of the most efficient combination alternatives - they enable the detection of any cycle slips configuration. This is now made possible thanks to the availability of data from Galileo's four carriers.

The quad-frequency algorithm has been tested on Galileo observations from both GMSD (Japan) and NKLG (Gabon) stations. On the first ones, cycle slips were artificially inserted in order to simulate particular cases and test algorithm robustness. NKLG raw data were used to assess algorithm behaviour for cases met in the equatorial area.

Enhanced with a suitable cycle slip correction method and a real-time feature, our algorithm could directly be integrated into the software receiver, enabling the supply of continuous and corrected data to the user.

In conclusion, this first quad-frequency cycle slips detection algorithm is obviously a step forward and every Galileo user will indeed be able to benefit from a highly better-quality positioning. With regard to precise positioning, this is yet another step reinforcing Galileo's competitivity against other dual or triple-frequency GNSS.

Keywords

GNSS, linear combination, four carriers, equatorial ionosphere, Galileo Open Service

1. Introduction

a. Context

The availability of data offered in *Open Service* on four carrier frequencies opens the way to new multi-frequency solutions for civil users. In this research, we focused on one of the consequences of signal track loss, i.e. cycle slips appearance.

Cycle slip detection is a key issue for high precision positioning application, from surveyors to aviation landing (security), precise farming and several military uses. Any user in need to determine a precise and reliable position must, at least, be aware of the presence of cycle slips in his data, since they compromise data quality. For instance, GNSS measurements use is growing in the surveyors' community. Indeed, more than ever, if a surveyor implants a building, he cannot afford any mistake in determining his own station position, which might then lead to a global shift in the building position.

Traditionally, two carrier frequencies were used for positioning, for instance GPS L1 and L2. More recently, three-carrier positioning allowed to enhance precision. Though using a third carrier frequency allowed to partially solve the cycle slip detection issue, existing procedures are still lacking in different aspects. One of today's main challenges is cycle slip detection under high ionospheric activity, which is why we focussed on this specific case study.

Since Galileo supplies four frequencies in *Open Service*, we might be able to improve once more cycle slip detection algorithm performances.

b. Framework

In this research a new quad-frequency cycle slip detection algorithm is introduced, an unexplored track in literature until now. The algorithm uses undifferenced carrier-phase observations from a single-station static receiver. At first developed for post-processing, the algorithm has also been adapted to real-time applications. This algorithm aims to improve cycle slips detection under high ionospheric activity.

First of all, we briefly explain what a cycle slip is and how it is obviously linked to phase observable (Sect. 2). Next, the quad-frequency algorithm is described in Sect. 3. Validation procedure and results follow in Sect. 4, before presenting perspectives and concluding in Sect. 5 and 6.

2. Cycle slip

a. Definition

Though code measurements are commonly used for average positioning, any precise positioning application needs to use carrier-phase measurements, due to their better quality. Unfortunately, the latter are potentially subject to cycle slip, generating a constant bias in data, thus impacting the inferred positioning.

Carrier-phase measurements are performed by observing the beat phase, i.e. the difference between the received carrier from the satellite and a receiver-generated replica. At the first observation epoch, only the fractional part of this beat phase can be measured, but the integer offset between satellite

signal and the receiver's replica is unknown. This integer number of cycles is called initial phase ambiguity and remains constant during the observation period.

The carrier-phase observable (between a satellite *i* and a receiver *p*), given in meters, is the following:

$$\phi_p^i[m] = G_p^i - I_{p,f_k}^i + M_{p,f_k,\phi}^i + HW + \lambda N_p^i + \varepsilon_{p,f_k,\phi}^i$$

where the subscript f_k indicates the term dependency on the frequency and ϕ on the carrier-phase observable. *G* is the geometric term (i.e. a function of the geometric range between the receiver and the tracked satellite, the tropospheric delay, and clock bias), I is the ionospheric delay, M is the multipath delay, *HW* stands for satellite and receiver hardware delays, N is the initial phase ambiguity, and ε is the random error (also called phase noise).

At the first observation epoch, an integer counter is initialised and as the tracking goes on it is incremented by one cycle whenever the beat phase changes from 2π to 0 [Hofmann-Wellenhof et al., 2008]. If the receiver – even briefly – loses the signal track, the counter is suspended and an integer number of cycles is lost. This loss can result from various causes (signal obstruction, high variability, etc.).

In the observation equation, the cycle slip will appear as a change in the value of the initial phase ambiguity. Thus, a one-cycle-amplitude slip will involve a phase measurement shift of about 20 cm (λ), depending on the affected carrier-frequency. The cycle slip size can vary from one to thousands of cycles.

Ionospheric delay is the only term that could possibly be confused with a small cycle slip. Indeed, during an ionospheric perturbation event, this delay variation between two observation epochs (in our case, every 30 seconds) often reaches more than 20 cm (i.e. the effect of one-cycle slip on the phase measurement). The ionosphere activity has two main consequences. Firstly, as mentioned before, slips can be hidden in observation noise and not detected. Secondly, received signal variability can cause loss of lock and thus cycle slips.

A lot of different configurations can arise when the signal is lost. Signal tracking can be interrupted on one single carrier (isolated cycle slip, ICS) or simultaneously on multiple carriers. In the second case, the slip magnitude on the different carriers concerned can be similar (simultaneous cycle slips of same magnitude, SCS-SM) or not (simultaneous cycle slips of different magnitude, SCS-DM).

b. Historically

The first cycle slip detection algorithm using undifferenced observation – Turbo Edit – was developed in 1990 [Blewitt, 1990]. Code and phase measurements from two carrier frequencies are used. It has been implemented in many data preprocessing program, such as GIPSY-OASIS II [Litchen, 1995], PANDA [Liu and Ge, 2003], and BERNESE [Beutler *et al*., 2007]. Turbo Edit algorithm has been enhanced numerous times. In its latest version [Cai *et al*., 2013], it was adapted to detect cycle slips under high ionospheric activity but is still dual-frequency.

Appearance of a third frequency allows to develop new combination of observables. A low-noise phase-only combination eliminating geometric as well as first-order ionospheric terms has been developed [Simsky, 2006] and applied for cycle slip detection [Lonchay et al., 2011]. Studies have also been made to determine the best combinations to be used in triple-frequency positioning [Feng, 2008],

and subsequently in cycle slip detection [Wu *et al*., 2009] and correction [Zhao *et al*., 2014] algorithms. These algorithms use both code and phase measurements, as well as triple-frequency method developed by de Lacy [de Lacy *et al.,* 2012].

Ionospheric concern is another new trend. In 2011, the *Total Electronic Content* rate was used to detect cycle slips [Liu, 2011]. Nevertheless, after studying ionospheric cycle slips, it was concluded that the "increased measurement noise associated with active ionosphere makes correcting cycles slips an ongoing challenge which requires further investigation" [Banville and Langley, 2013]. Zhang came to an identical conclusion while trying to repair cycle slips during scintillation event [Zhang *et al.*, 2014].

3. Quad-frequency algorithm

Cycle slip detection techniques use testing quantities (where the cycle slip is represented by a jump). Those are associated to a discontinuity detection algorithm, which aims to locate this jump.

a. Testing quantities

Testing quantities are linear combinations of observations. They differ in several aspects: the observables used (in our case, only phase measurements), the number of carrier frequencies used, and combination inner properties (geometry-free, ionosphere-free, and noise level on the combination).

Further in our study, we will assume the noise on carrier-phase measurements is the following [Springer and Schönemann, 2013]:

Carrier	Central frequencies [MHz]	Carrier-phase measurement noise [m]
E1	1575.420	0.0030
E5a	1176.450	0.0016
E5b	1207.140	0.0016
E5a+b	1191.795	0.0008

Table 1 : Galileo frequencies available in Open Service

i. Triple-frequency Simsky combination

Our algorithm is mainly based on triple-frequency Simsky combination exploitation. It is a geometry-free and ionosphere-free carrier-phase combination [Simsky, 2006].

$$S_p^i\,[m] = \left(\frac{\lambda_{f_3}^2 - \lambda_{f_2}^2}{\lambda_{f_2}^2 - \lambda_{f_1}^2}\right)\phi_{p,f_1}^i + \left(\frac{\lambda_{f_1}^2 - \lambda_{f_3}^2}{\lambda_{f_2}^2 - \lambda_{f_1}^2}\right)\phi_{p,f_2}^i + \phi_{p,f_3}^i$$

When four frequencies are available, four triple-frequency combinations can be computed. Two of them are sufficient to detect slips on any of the four frequencies.

The combination choice must first depend on its precision (Table 2, σ_S), obtained by applying the variance-covariance propagation law to raw measurement noise (Table 1). Precision is not the only factor to be taken into account in the choice of suitable combinations. In each combination, carrier

frequencies have different impacts due to their different wavelengths: the impact of a one-cycle-amplitude slip on E1 frequency will indeed not be the same as the one on E5a, E5b, or E5a+b (Table 2). The smallest impact on a given combination is always the most difficult one to detect.

Carriers used	Simsky combination precision (σ_S) [m]	Smallest impact [m]
E1 ; E5a ; E5b	0.0024	(E1) 0.024
E1 ; E5a ; E5a+b	0.0018	(E1) 0.012
E1 ; E5b ; E5a+b	0.0019	(E1) 0.012
E5a ; E5b ; E5a+b	0.0028	(E5a) 0.255

Table 2 : Simsky combinations

Therefore, the efficiency of a given combination will depend on both the effect of the smallest cycle slip and the combination precision (given by the standard deviation): the higher the ratio between them, the more efficient the combination (Figure 1).

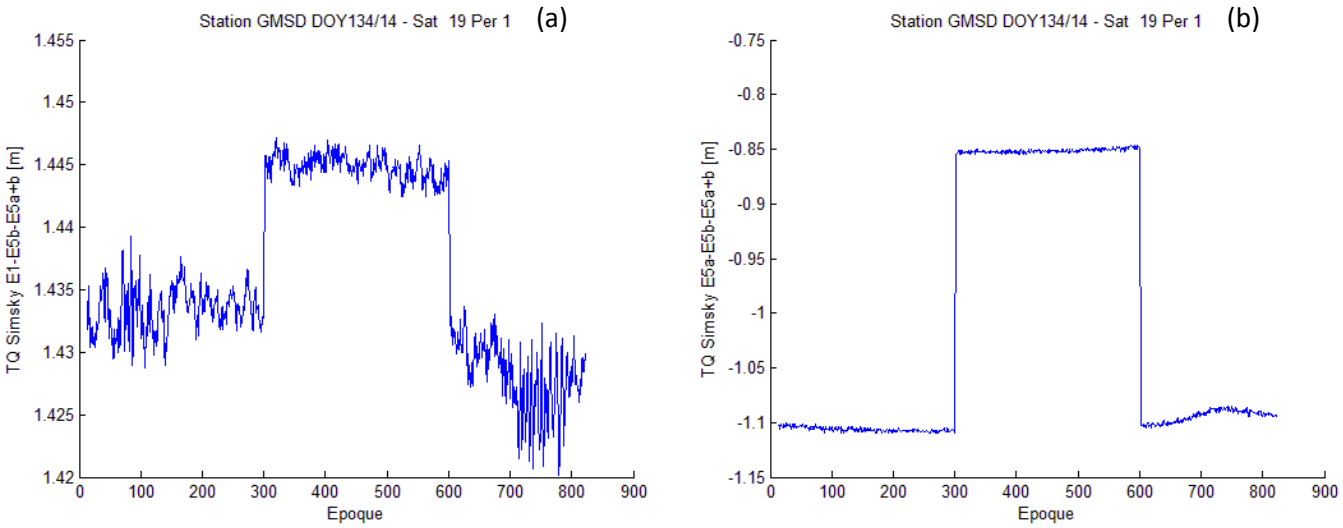

Figure 1: 1-cycle slip on E1 on Simsky E1-E5b-E5a+b combination (a) and 1-cycle slip on E5a on E5a-E5b-E5a+b combination (b)

Among those four combination possibilities, the highest two ratios are held by E5a-E5b-E5a+b and E1-E5a-E5b combinations, these will thus be the ones used in our algorithm.

The Simsky combination allows to detect ISC as well as SCS-DM. Nevertheless, this combination is insensitive to SCS-SM on all four frequencies (mainly limited to receiver failures during data processing). We will thus have to add another testing quantity in our algorithm.

ii. Dual-frequency Geometry-free combination

Dual-frequency GF combination allows to detect SCS-SM. It can be computed as follows:

$$GF_p^i\ [m] = \phi_{p,f_1}^i - \phi_{p,f_2}^i$$

Unfortunately, raw dual-frequency Geometry-free combination is affected by ionospheric delay. In order to mitigate ionospheric smooth trend, fourth-order time difference is computed. Still, the result suffers from quick variation of ionospheric delay.

When four frequencies are available, six dual-frequency combinations can be computed. One is sufficient to detect the presence of simultaneous cycle slips of the same magnitude. The choice will again depend on the ratio between combination precision and the smallest effect of simultaneous one-cycle slip.

On the one hand, differencing the combination results affects precision. On the other hand, the cycle slip, thus the smallest effect to detect, will be amplified by high-order differencing. The best ratio is obtained with fourth-order difference (Table 3), even if smooth ionospheric variation will be compensated from second-degree differencing (Figure 2).

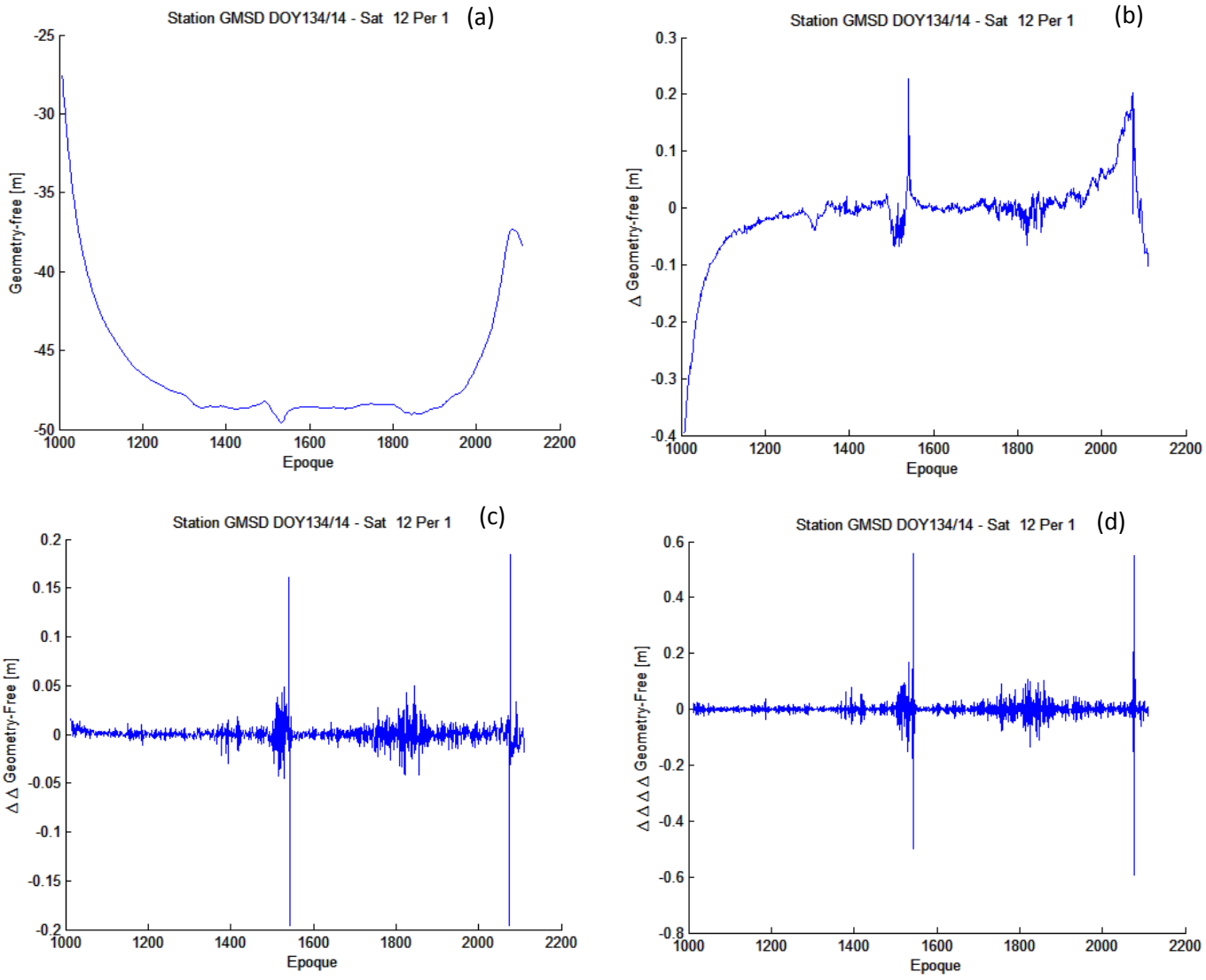

Figure 2: Time-differenced Geometry-Free combination: raw combination (a), 1st order difference (b), 2nd order difference (c), 4th order difference (d).

Carriers used	(Fourth-order differenced) Geometry-Free combination precision (σ_{GF}) [m]	Smallest effect SCS-SM = 1 cycle [m]
E1 ; E5a	0.0136	0.1935
E1 ; E5b	0.0136	0.1740
E1 ; E5a+b	0.0124	0.1836
E5a ; E5b	0.0091	0.0195
E5a ; E5a+b	0.0072	0.0099
E5b ; E5a+b	0.0072	0.0096

Table 3 : Geometry-Free combinations

Even if one combination is sufficient, we will use two of them in order to overlap their outputs: E1-E5a and E1-E5a+b, since they offer the best ratios.

b. Detection method

To detect discontinuity in the testing quantity, it is necessary to fix thresholds. Thresholds are one of the key parameters in cycle slips detection, since they lead to the decision of a cycle slip presence or not. If the threshold is too restrictive, some real slips can be missed (*false negative*). On the opposite, if it is not restrictive enough, some discontinuities which do not match with a cycle slip could be abusively detected (*false positive*).

It is important to notice, as our study highlights, that there is no perfect threshold allowing to suit all the needs and constraints. The choice must be made considering the application behind positioning. Threshold values given in this paper are indicative and were empirically determined to be optimal with respect to our goal (detection under high ionospheric activity). Results and further discussions about different thresholds can be found in [Van de Vyvere, 2015].

Cycle slips will affect raw combination by a shift in average whereas the time-differenced one will be affected by a peak (Figure 3).

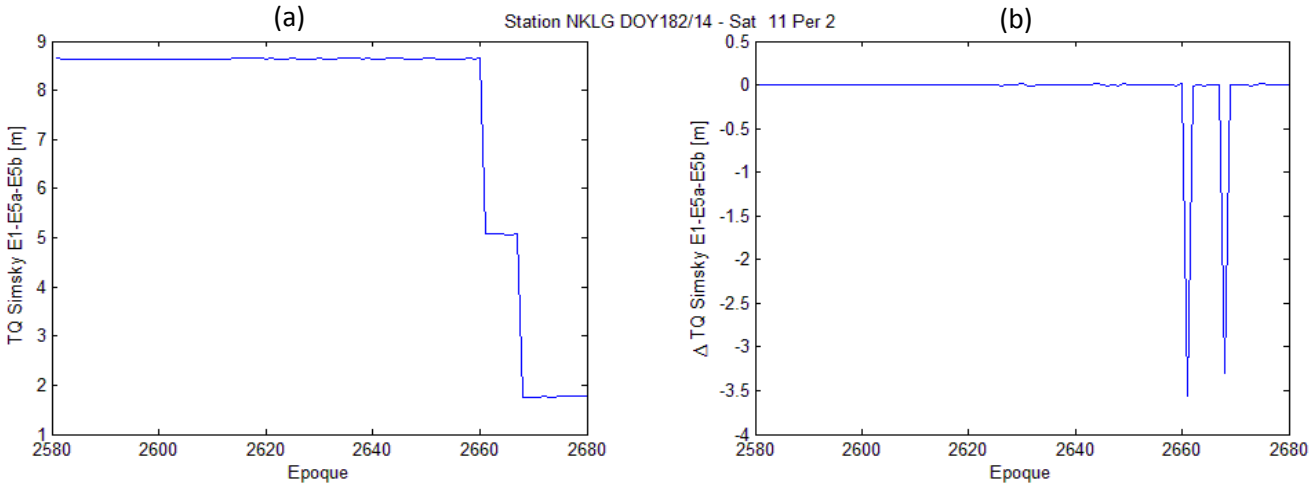

Figure 3: Cycle slips effect on raw (a) and differenced (b) Simsky combination

i. Detection on Simsky combination

Cycle slip detection on triple-frequency Simsky combination is performed in two cascading steps (Figure 4).

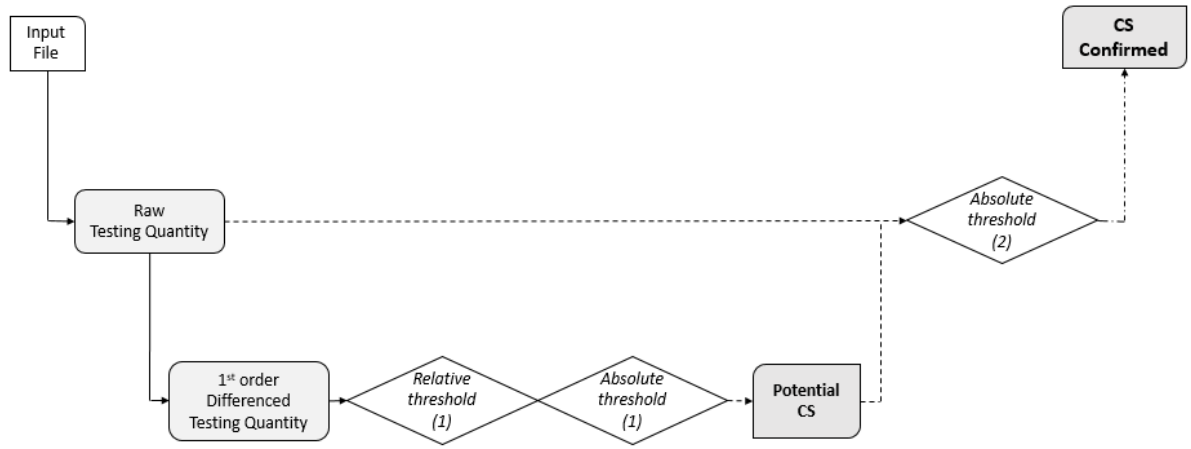

Figure 4 : Detection method on Simsky combination

The first one uses a time-differenced combination to detect potential cycle slips using a 20-observation-sized forward and backward moving average window, in which statistical parameters as average and standard deviation are computed. The current epoch is compared to the previous ones in order to detect a peak which could correspond to a cycle slip. Two types of thresholds are used: statistical (or relative) and absolute.

As shown in Figure 5, using a *statistical threshold* allows to adapt detection to the inertia of statistical parameters. Assuming the observations (here, the Simsky combination results) follows a Normal Distribution, a confidence interval of 3σ around average includes 95 % of observations. Given the ratio of the two Simsky combinations used (computed earlier), the success rate reaches 100 % for both combinations, which means any ICS and SCS-DM on data will be detected for sure (no false negatives). Nevertheless, *false positives* may occur since 5% of data are statistically out of bounds.

In order to reduce this rate, an *absolute threshold* is also applied, valued to 0.4 multiplied by the smallest impact of a cycle slip on the combination. If Figure 5 is a suitable example of an extreme ionospheric disturbance leading to unusual high variability in combination results, the absolute threshold will most of the time be far higher than the statistical one and will help to reduce the rate of wrong detections.

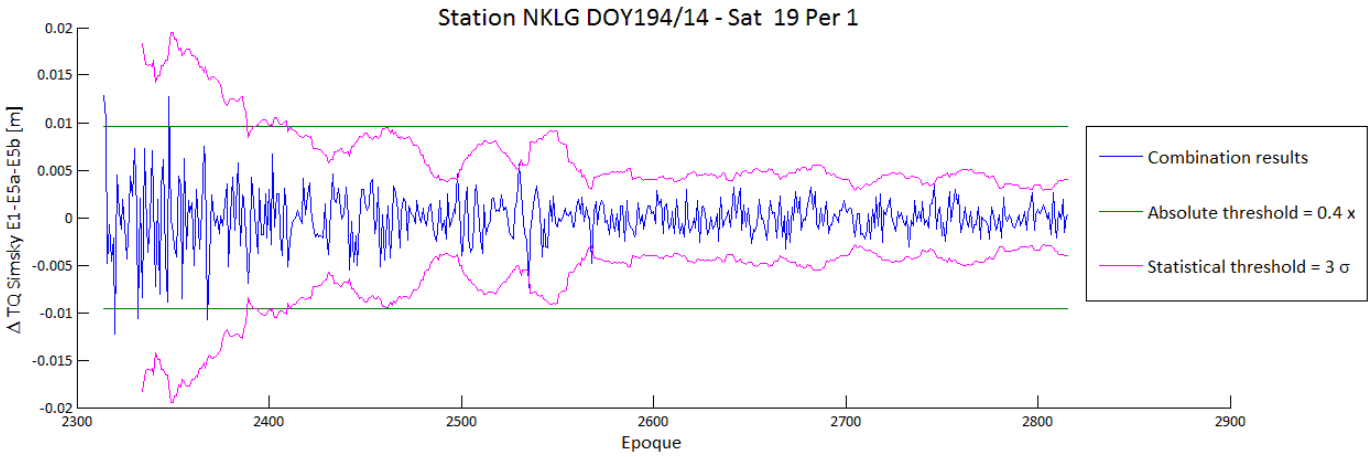

Figure 5: Statistical and absolute thresholds

As an output of this first step, a flag value is assigned to epochs which are superior to both thresholds, thus potentially affected by cycle slips.

Once the location of potential jumps is achieved, the second step consists in comparing the average before and after potential cycle slips for the flagged epochs. A second absolute threshold is applied, valued to 0.8 multiplied by the smallest effect. If another potential cycle slip is present in the detection window, the latter will be reduced in order to avoid statistical parameters calculation on partially shifted data.

The goal of the first step is to detect potential slips: thus the priority is to avoid missing a real slip, with low threshold values, sometimes leading to false positive detection. Oppositely, the second step aims to separate the potential remaining false positives – outlier peaks in the raw combination – from the real cycle slips - shifts in average. The theoretical performance of this two-step approach is 100 %: neither *false positives* nor *false negatives* should be encountered.

ii. Detection on Geometry-Free combination

Since fourth-order differenced Geometry-Free combination is affected by a residual ionospheric delay, the previous procedure cannot be applied. Like any time-differenced testing quantity, the slip will appear as a peak in the combination. Therefore, there is no way to distinguish them from outliers by an average comparison (second step).

Thus, the detection method only consists in a forward-and-backward moving average window, in which a 4σ confidence interval is compared to the current epoch combination value. Indeed, in this case, we cannot afford to encounter *false positives* on 5% of epochs (induced by the use of a 3σ threshold) since no further step can be set up in order to eliminate remaining *false positives*.

The theoretical performances of the Geometry-Free detection method are also expected to reach 100%: again, neither *false positives* nor *false negatives* should be encountered. Note that this calculation only takes ratio into account, neglecting the sensitivity to ionosphere.

4. Validation

a. Data and methodology

The quad-frequency algorithm has been tested on 30-second quad-frequency Galileo observations from both GMSD (Japan) and NKLG (Gabon) stations, all of them using Trimble NetR9 receiver. GMSD observations are used to test algorithm robustness towards simulated particular cases, whereas NKLG data set assess algorithm behaviour for cases met in the equatorial area.

In GMSD data, cycle slips were previously artificially inserted, simulating the following scenarios: ICS, SCS-DM and SCS-SM. The benefit of such a simulation approach is that the algorithm output can easily be compared to the already known solution. Moreover, these data had been used to determine whether the use of more carrier frequencies could increase cycle slips detection performance or not (demonstrated in [Van de Vyvere, 2015]).

A total of 50-day NKLG data set, covering observation from 6th January to 1st February and from 24th June to 19th July 2014, were analysed. This sample is made up of various ionospheric states: calm or extreme days, as well as typical equatorial activity. Since the climax of our solar cycle happened in 2014, data from that year perfectly fit a study under high ionospheric activity.

NKLG raw data were used in order to achieve a dual goal.

At first, we wanted to determine the proportion of epochs in which small cycle slips (1, 2, or 5 cycles of amplitude) wouldn't be able to be distinguished. This was performed by comparing the impact (in meters) of such scenarios to the instantaneous threshold associated with each epoch. In the case of a superior threshold, then potentially present slips of 1, 2, or 5 cycles couldn't be detected. The daily proportion of the previously mentioned epochs - for each combination used in the algorithm - seemed to be a suitable indicator of algorithm effectiveness in the equatorial area.

At second, we analysed results by visually assessing algorithm output using combinations graphics (Figure 6), and tried to answer to the following questions: Do flagged epochs seem to be affected by cycle slips? Are there actual cycle slips which remain undetected?

Two epochs are detected on Simsky combinations (red lines, Figure 6.a and 6.b). They obviously match real cycle slips. An influence of these slips is also observable on Geometry-Free combinations (Figure 6.c and 6.d).

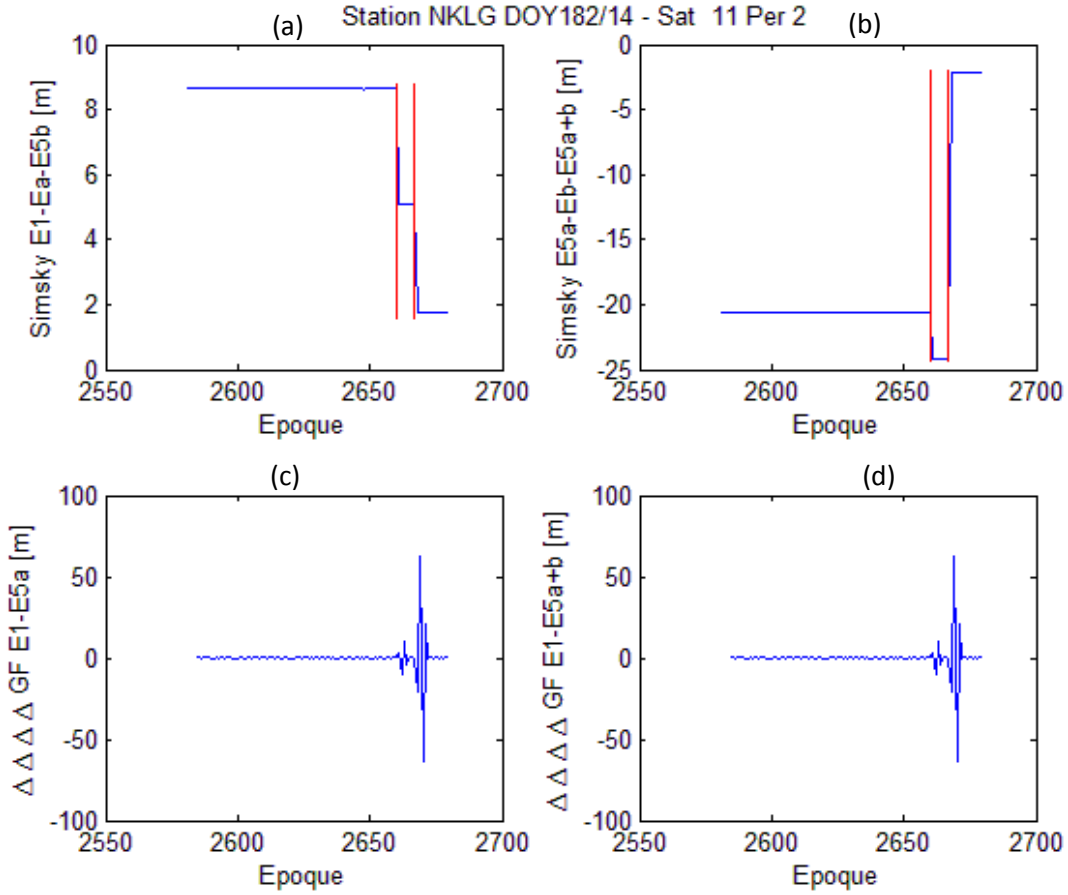

Figure 6: Algorithm graphical output

b. Results

i. Particular cases simulation

Compared to equivalent dual and triple-frequency methods, this new quad-frequency algorithm gave better results: all inserted cycle slips were successfully detected and no *false positive* were noticed. Performances amelioration is demonstrated in [Van de Vyvere, 2015].

ii. NKLG raw data set analysis

The validation process using NKLG raw data highlights several trends in algorithm results.

First of all, it is interesting to notice that the detection of isolated slips as well as slips of different magnitude (using Simsky combinations) was guaranteed for every observation epoch of every analysed day. Indeed, Simsky instantaneous thresholds never exceeded the effect of a slip of one-cycle-amplitude.

In addition, in 25 % of the analysed days, detection of cycle slips of the same magnitude could also be guaranteed. For the remaining days, detection of simultaneous cycle slips whose amplitudes are less than 5 cycles could not be guaranteed for a few observation epochs, which can reasonably be

neglected because of the very small probability to meet such exceptional cases. This is due to the impact of ionospheric variability in Geometry-Free combination, inducting high instantaneous threshold values.

However, both Simsky and Geometry-Free combinations suffer from *false positive* detection under extreme ionospheric events: if a cycle slip is detected, it sometimes corresponds to an outlier. This side effect is due to the threshold choices we made to match our initial purpose: detecting all cycle slips for sure, rather than risking to miss any one of them, even if *false positives* are part of the results list.

5. Further improvements

Next to post-processing application, a real-time adaptation of the algorithm has also been considered. This real-time constraint both impacts Simsky and Geometry-Free detection methods. In this configuration, the statistical window can indeed only move forward, which neglects cycle slips detection on the first twenty epochs. Further on, average comparison (see *Simsky detection method*) can no longer be considered since the average following the potential cycle slip cannot be computed in real-time processing. If our quad-frequency detection algorithm could therefore suffer from real-time constraint, it still proves efficient if the latter is taken into account for suitable thresholds choices.

If being aware of a cycle slip presence in his data is a precious information for the user, it does not prevent him from reinitialising several parameters. Detection is indeed only a first step, and cycle slip correction should complete the procedure to avoid discontinuity. If a theoretical solution is ready, the correction algorithm validation is currently being set up.

Enhanced with a suitable cycle slip correction method and a real-time feature, our algorithm could directly be integrated into the software receiver, enabling the supply of continuous and corrected data to the user.

6. Conclusion

In this paper, we introduced the first quad-frequency cycle slips detection algorithm, whose efficiency is obviously a step forward compared to previous ones.

This innovative detection method opens new doors to numerous research and commercial applications. Every Galileo user - civil or military - will indeed be able to benefit from a highly better-quality positioning, especially in harsh conditions: not only where ionosphere is particularly restless like equatorial and polar areas, but also at any latitude during ionospheric disturbance.

With regard to precise positioning, this is yet another step reinforcing Galileo's competitivity against other dual or triple-frequency GNSS.

References

- [Banville and Langley, 2013] Banville, S. and Langley, R. (2013). Mitigating the impact of ionospheric cycle slips in GNSS observations. *Journal of Geodesy*, 87:179-193.

- [Beutler et al., 2007] Beutler, G., Bock, H., Dach, R., Fridez, P., Gäde, A., Hugentobler, U., Jäggi, A., Meindl, M., Mervart, L., Prange, L., Schaer, S., Springer, T., Urschl, C., and Walser, P. (2007). *Bernese GPS Software Version 5.0.* Astronomical Institute, University of Bern.

- [Blewitt, 1990] Blewitt, G. (1990). An automated editing algorithm for GPS data. *Geophysical Resarch Letter*, 17(3):199-202.

- [Cai et al., 2013] Cai, C., Liu, Z., Xia, P., and Dai, W. (2013). Cycle slip detection and repair for undifferenced GPS observations under high ionospheric activity. *GPS Solutions*, 17(2):247-260.

- [de Lacy et al., 2012] de Lacy, M., Reguzzoni, M., and Sanso, F. (2012). Real-time cycle slip detection in triple-frequency GNSS. *GPS Solutions*, 16(3):353-362.

- [Feng, 2008] Feng, Y. (2008). GNSS three carrier ambiguity resolution using ionosphere-reduced virtual signals. *Journal of Geodesy*, 82(12):847-862.

- [Hofmann-Wellenhof et al., 2008] Hofmann-Wellenhof, B., Lichtenegger, H., and Wasle, E. (2008). *Global Navigation Satellite Systems: GPS, GLONASS, Galileo & more*, 194-202. Springer-Wien New York.

- [Litchen, 1995] Litchen, S. (1995). GISPY OASIS II: a high precision GPS data processing system and general orbit analysis tool. In *Technology 2006, NASA Technology Transfer Conference*, Chicago, Illinois.

- [Liu and Ge, 2003] Liu, J.-N. and Ge, M.-R. (2003). PANDA software and its preliminary result of positioning and orbit determination. *Wuhan University Journal of Natural Sciences*, 8(2B):603-609.

- [Liu, 2011] Liu, Z. (2011). A new automated cycle slip detection and repair method for a single dual-frequency GPS receiver. *Journal of Geodesy*, 85(3):171-183.

- [Lonchay et al., 2011] Lonchay, M., Bidaine, B., and Warnant, R. (2011). An efficient dual and triple frequency preprocessing method for Galileo and GPS signals. In *Proceedings of the 3rd international colloquium-scientific and fundamentals aspects of the GALILEO programme*, Copenhagen, Denmark.

- [Simsky, 2006] Simsky, A. (2006). Three's the Charm - Triple Frequency Combinations in Future GNSS. *Inside GNSS*, 5:38-41.

- [Springer and Schönemann, 2013] Springer, T. and Schönemann, E. (2013). GNSS analysis in multi-GNSS and multi-signal environment. In *American Geophysical Union Meeting*.

- [Van de Vyvere, 2015] Van de Vyvere, L. (2015). Détection des sauts de cycles en mode multi-fréquence pour le système Galileo. Master's thesis, Université de Liège.

- [Wu et al., 2009] Wu, Y., Jin, S., Wang, Z., and Liu, J. (2009). Cycle slip detection using multi-frequency GPS carrier phase observations: a simulation study. *Advances in Space Research*, 46(2):144-149.

- [Zhang et al., 2014] Zhang, X., Guo, F., and Zhou, P. (2014). Improved precise point positioning in the presence of ionospheric scintillation. *GPS Solutions*.

- [Zhao et al., 2014] Zhao, Q., Sun, B., Dai, Z., Hu, Z., Shi, C., and Liu, J. (2014). Real-time detection and repair of cycle slips in triple-frequency GNSS measurements. *GPS Solutions*.